

Omental adipocyte hypertrophy relates to coenzyme Q10 redox state and lipid peroxidation in obese women^S

Thomas Grenier-Larouche,^{1,*†} Anne Galinier,^{1,§,*,†,§§} Louis Casteilla,^{§,*,†,§§}
André C. Carpentier,[†] and André Tchernof^{2,*}

Endocrinology and Nephrology Axis,* Centre Hospitalier Universitaire de Québec, Québec, Canada; Department of Medicine, Division of Endocrinology,[†] Université de Sherbrooke, Québec, Canada; CNRS 5273, UMR STROMALab,[§] Toulouse, France; Université de Toulouse, UPS,^{**} Toulouse, France; INSERM U1031,^{††} Toulouse, France; and EFS Pyrénées-Méditerranée,^{§§} Toulouse, France

Abstract Occurrence of oxidative stress in white adipose tissues contributes to its dysfunction and the development of obesity-related metabolic complications. Coenzyme Q10 (CoQ10) is the single lipophilic antioxidant synthesized in humans and is essential for electron transport during mitochondrial respiration. To understand the role of CoQ10 in adipose tissue physiology and dysfunction, the abundance of the oxidized and reduced (CoQ10_{red}) isoforms of the CoQ10 were quantified in subcutaneous and omental adipose tissues of women covering the full range of BMI (from 21.5 to 53.2 kg/m²). Lean women displayed regional variations of CoQ10 redox state between the omental and subcutaneous depot, despite similar total content. Obese women had reduced CoQ10_{red} concentrations in the omental depot, leading to increased CoQ10 redox state and higher levels of lipid hydroperoxide. Women with low omental CoQ10 content had greater visceral and subcutaneous adiposity, increased omental adipocyte diameter, and higher circulating interleukin-6 and C-reactive protein levels and were more insulin resistant. The associations between abdominal obesity-related cardiometabolic risk factors and CoQ10 content in the omental depot were abolished after adjustment for omental adipocyte diameter. **■** This study shows that hypertrophic remodeling of visceral fat closely relates to depletion of CoQ10, lipid peroxidation, and inflammation.—Grenier-Larouche, T., A. Galinier, L. Casteilla, A. C. Carpentier, and A. Tchernof. Omental adipocyte hypertrophy relates to coenzyme Q10 redox state and lipid peroxidation in obese women. *J. Lipid Res.* 2015. 56: 1985–1992.

Supplementary key words adipose tissue • obesity • adipocytes • antioxidant • mitochondria • ubiquinol • ubiquinone • body fat distribution • cardiometabolic risk factors

The metabolic consequences of excess fat accumulation, especially in intra-abdominal adipose tissue compartments,

This work was supported by operating funds from the Canadian Institutes of Health Research, Institute of Gender and Health (MOP-64182) (A.T.). A. Tchernof is codirector of a Research Chair in Bariatric and Metabolic Surgery. A. C. Carpentier is the director of the CIHR-GSK Chair in diabetes. The authors have declared no conflict of interest exists related to the content of this article.

Manuscript received 13 February 2015 and in revised form 13 July 2015.

Published, JLR Papers in Press, August 3, 2015
DOI 10.1194/jlr.P058578

are closely related to white adipose tissue dysfunction. This phenomenon is characterized by adipocyte hypertrophy, inflammatory cytokine secretion, and altered postprandial lipid fluxes (1). A growing body of evidence suggests that oxidative stress might be involved early in this pathological state. In white adipocytes, reactive oxygen species (ROS) production is mainly driven by NADPH oxidase activity instead of xanthine oxidase or mitochondrial respiration (2). Moreover, a reduction in expression levels and activity of antioxidant enzymes, like superoxide dismutase (SOD), glutathione peroxidase (GPx), and catalase, was observed in obesity (2). This phenomenon suggests that greater formation of toxic byproducts, derived from lipid peroxidation and the protein carbonylation process, occurs during the synthesis of hydrogen peroxide or 4-hydroxy-2-nonenal (4-HNE). These byproducts impair adiponectin secretion (3) and increase cytokine production by mature adipocytes (2). Exposure to 4-HNE also promotes lipolysis (4) and induces insulin resistance in skeletal muscle (5, 6).

Coenzyme Q10 (CoQ10) is a molecule at the crossroad of mitochondrial metabolism and ROS detoxification. It is the most prevalent form of coenzyme Q (CoQ) in humans. It is ubiquitous and present under three different redox states: fully oxidized (ubiquinone, CoQ10_{ox}), fully reduced (ubiquinol, CoQ10_{red}), and the semiquinone radical (7). CoQ10 is mostly found in cellular membranes because of the lipophilic properties of the isoprenoid tail. Its biosynthetic pathway mainly occurs in mitochondria, where the

Abbreviations: CoQ, coenzyme Q; CoQ10, coenzyme Q10; CoQ10_{ox}, oxidized coenzyme Q10; CoQ10_{red}, reduced coenzyme Q10; CoQ10_{tot}, total coenzyme Q10; COQ2, coenzyme Q2 4-hydroxybenzoate polyprenyltransferase; CRP, C-reactive protein; CT, computed tomography; IL-6, interleukin-6; LPO, lipid hydroperoxide; ROS, reactive oxygen species.

¹T. Grenier-Larouche and A. Galinier contributed equally to this article.

²To whom correspondence should be addressed.

e-mail: andre.tchernof@crchul.ulaval.ca

S The online version of this article (available at <http://www.jlr.org>) contains a supplement.

condensation of the isoprenyl side chain with the benzoquinone nucleus is catalyzed by the coenzyme Q2 4-hydroxybenzoate polyprenyltransferase (COQ2) enzyme (8). This is the cellular compartment with the highest concentration, where it shuttles electrons from complexes I and II to complex III during oxidative phosphorylation (7, 9). Moreover, CoQ10 has been shown to modulate the activity of uncoupling protein (9). CoQ10 was also found in the Golgi apparatus, the endoplasmic reticulum, and plasma membrane (10). The extra mitochondrial CoQ10 pool is involved in plasma membrane electron transport catalyzed by NAD(P)H-dependent enzymes (11). Moreover, the reduced isoform displays direct or indirect antioxidant properties by scavenging lipid peroxy radical or by reducing α -tocopherol (12).

Depletion of CoQ10 content was found in subcutaneous adipose tissue of obese subjects and mice (13). Overexpression of COQ2 in 3T3-F442A preadipocytes decreased the CoQ redox state and promoted ROS synthesis by the mitochondria (13). Interestingly, the adipogenic potential of these cells was almost completely blunted, suggesting an important role of CoQ content and redox state during adipogenesis and adipose tissue expansion. However, the variation in CoQ10 content and redox state in subcutaneous and omental adipose tissues has not been investigated in humans. Moreover, the potential contribution of these parameters to white adipose tissue dysfunction and obesity-related metabolic complications remains unclear.

In the present study, we have explored physiological variations in CoQ10 content and redox state in omental and subcutaneous adipose tissue of lean, overweight, and obese women. We hypothesized that CoQ10_{red} content is lower in omental fat of obese individuals and is associated with lipid peroxidation. The loss of lipophilic antioxidant capacity of this molecule could be an important mechanism. We also postulate that this phenomenon could link visceral adipose tissue hypertrophy to systemic low-grade inflammation and insulin resistance.

MATERIALS AND METHODS

Participants

Women undergoing elective hysterectomy (n = 29) without (n = 17) or with unilateral (n = 4) or bilateral (n = 8) salpingo-oophorectomy were recruited at the gynecologic unit of the Laval University Medical Center. Surgery was performed for the following reasons: menorrhagia/menometrorrhagia (n = 9), myoma/fibroids (n = 15), incapacitating dysmenorrhea (n = 1), pelvic pain (n = 1), benign cyst (n = 5), endometriosis (n = 2), pelvic adhesions (n = 1), hypermenorrhea (n = 1), excessive anemia-causing uterine bleeding (n = 1), endometrial hyperplasia (n = 2), or polyp (n = 2). All scientific protocols were approved by the Research Ethics committee of Laval University Medical Center. Subjects provided written informed consent before their inclusion in the study.

Adipose tissue sampling

Subcutaneous adipose tissue samples were collected at site of the surgical incision (lower abdomen), while omental samples were removed from the distal part of the greater omentum. Fresh

samples were immediately carried to the laboratory and used for adipocyte isolation. A portion of each sample was flash frozen in liquid nitrogen and stored at -80°C .

Adipocyte isolation and cell sizing

Tissue samples were digested with collagenase type I in Krebs-Ringer-Henseleit buffer for 45 min at 37°C according to a modified version of the Rodbell method (14–16). Cell suspensions were filtered through nylon mesh and washed three times with Krebs-Ringer-Henseleit buffer. To determine adipocyte diameter, pictures of 250 cells were taken with a phase contrast microscope and analyzed with Scion Image software. The collagenase digestion was not performed for three samples because of the limited amount of tissue.

Measurement of body composition and adipose tissue distribution

The determination of body fat and lean body mass was performed by dual-energy X-ray absorptiometry (DEXA) using a Hologic QDR-2000 densitometer and the enhanced array whole-body software V5.73A (Hologic, Bedford, MA). Regional adipose tissue distribution was measured by computed tomography (CT) as previously described (14, 17) using a GE Light Speed 1.1 CT scanner (General Electric Medical Systems, Milwaukee, WI). Briefly, the cross-sectional scan was performed at the L4–L5 vertebrae level in supine position with arms over the head. The exact scanning position was determined using a scout image. Adipose tissue areas of interest including visceral and subcutaneous adipose tissue areas, the latter included superficial and deep subcutaneous adipose tissues, were highlighted and computed with attenuation ranging from -190 to -30 Hounsfield units with ImageJ 1.33u software (National Institutes of Health, Bethesda, MD). Two obese volunteers exceeded the CT scanner field of view, and only the visceral adipose tissue area was determined. One of these women also exceeded the upper limit of weight allowed for the DEXA table and did not undergo this test.

Quantification of lipid hydroperoxide levels in white adipose tissues

Lipid hydroperoxides (LPOs) were quantified using an LPO assay kit purchased from Cayman Chemical (Ann Arbor, MI), performed according to supplier recommendations with minor modifications. Briefly, 50 mg of omentum and subcutaneous adipose tissues were homogenized in methanol. Lipid extraction was achieved by adding 500 μl of water and 1 ml of chloroform. The mixture was centrifuged at 1,500 g and the organic phase was collected. An aliquot was used to perform the colorimetric reaction, and absorbance was read at 500 nm with a 96-well plate reader.

Quantification of CoQ10 isoforms

The quantification of both isoforms was performed by reverse-phase HPLC with electrochemical detection as previously described (18). The HPLC-EC system is composed of a Gilson 307 pump, a Rheodine injector, an analytical column, and an ESA Coulochem 2 Electrochemical Detector (Model 5200 A) with a computer/controller with EuroChrom 2000 Integration Package. The analytical cell (ESA Model 5010 porous graphite) consisted of a series of two coulometric electrodes and was connected in series to the analytical column: the first electrode (E2) was for reduction of CoQs, and the second electrode (E3) was for detection of these reduced CoQs. The identification of the different forms was set by the chromatographic separation with an analytical column, a reverse-phase Hypersil BDS C18 column (4 mm \times 25 cm, 5 μm bead). The mobile phase for the isocratic elution of internal standard from ChromSystem and CoQ10s containing

sodium acetate, acetic acid and 2-propanol, methanol and hexane, suited for EC detector. The standards of CoQ10_{ox} were obtained from Sigma. Identification and quantification of oxidized and reduced forms of CoQs were performed using in-house external standards. The concentration of the working solution was confirmed by measuring absorbance at a wavelength of 275 nm and by reference to known coefficients ($E_{1\text{cm}}^{1\%}$ 185 for CoQ9 and 165 for CoQ10). Then the conditioned solution of oxidized standard was reduced in loop to $-1,000$ mV in the system pump-guard cell. The determination of the concentration of each form was compared with the QA program organized by the National Institute of Standard Technology on lyophilized serums. Calibration curves were performed with a mix of three different diluted working CoQ10s stock solutions. Before injection, each standard solution was prepared as the biological samples in propanol. A highly linear relationship was observed between the area of the peak (mV/min) and the molecular concentration ratios of each compound over a wide concentration from 10–15 nM to 3,000 nM ($r = 0.99$). Acceptable repeatability was obtained for CoQs with a coefficient of variation below 5%, respectively 3.5% and 3.7% for CoQ10_{red} and CoQ10_{ox}. The limits of detection per injected quantity were 21 pmol for CoQ_{red} and 15 pmol for CoQ_{ox}.

To perform CoQ10 extraction, frozen tissues (100 mg) were added to 0.9 ml of 2-propanol and homogenized with an Ultraturax blender. One hundred microliters of this homogenate was mixed with 500 μ l of 2-propanol during 30 s and then centrifuged (10,000 rpm for 3 min). Fifty microliters of the supernatant was directly injected in the system. This extraction procedure with only propanol was chosen because it was simple to perform and avoid oxidation of reduced CoQ forms as it was demonstrated and validated using various molecules well known to modify electron flow at different levels of the respiratory chain. As expected, CoQ redox state was significantly decreased in the presence of antimycin A and significantly increased in the presence of rotenone and carbonyl cyanide *m*-chlorophenyl hydrazone. The details of the validation were reported by Galinier et al. (18). The total coenzyme Q10 (CoQ10_{tot}) pool was described as the sum of CoQ10_{ox} and CoQ10_{red} concentrations. Results were expressed as nmol/g of tissue. The redox state was calculated as follows: $[\text{CoQ10}_{\text{ox}}]/[\text{CoQ10}_{\text{tot}}] \times 100$.

Estimation of daily dietary CoQ10 consumption

Dietary intake was assessed using a food frequency questionnaire validated by Goulet et al. (19) that was interviewer administered by the same investigator within 2 weeks preceding or following the surgery and was structured to represent food habits throughout the previous month. The questionnaire was based on foods available in the Quebec City area and reflected Canadian food habits. The participants were questioned about the quantity and frequency intake of each item among different food groups: vegetables, fruits, legumes, nuts and seeds, cereals and grain products, milk and dairy products, meat/processed meat, poultry, fish, eggs, sweets, oil and fats, fast foods, and drinks. The content in CoQ10 by portion of each food groups was estimated using the compiled by Pravst et al. (20) and is reported in supplementary Fig. 1. Total daily consumption of CoQ10 was calculated as the sum from each food source.

Statistical analyses

All tables show mean \pm standard error of the mean. Each graph shows dots as a single observation and horizontal lines as the mean of the distribution. Differences among body weight categories and adipose tissue depots were analyzed by two-way ANOVA, followed by Tukey's post hoc test. The stratification of CoQ10 content in the omental and subcutaneous depot was performed using a cutoff value of 14.0 and 15.0 nmol/g of tissue, respectively. These values

were selected from a previous publication (13). Differences between women with low and high concentrations of CoQ10 were analyzed by Student's *t*-test or Mann-Whitney test. Multiple univariate Pearson's linear correlations were performed to find associations between adiposity measurements and the concentrations of the CoQ10 isoforms for both depots. Log10 and Box-Cox transformations were used for correlations with nonnormally distributed residuals. Statistically significant correlations (in omental depot) between body fat distribution parameters and CoQ10 isoforms were adjusted for omental fat cell diameter to investigate the confounding effect of visceral fat hypertrophy. Statistical analyses were performed with the JMP 11.0 (SAS Institute, Cary, NC) and GraphPad Prism 6 (GraphPad, a Jolla, CA) software.

RESULTS

Volunteer characteristics

Twenty-nine Caucasian women aged between 40.4 and 55.5 years (mean of 48.1 ± 4.1) were recruited. Their anthropometric and metabolic characteristics are shown in **Table 1**. They were characterized by a wide range of BMI values (from 21.5 to 51.3 kg/m²) with an average around the class I obesity threshold (30.0 ± 6.8 kg/m²). Of the 29 volunteers, 7 were lean (BMI <25.0 kg/m²), 12 were overweight (BMI 25.0 kg/m² to 30.0 kg/m²), and 10 were obese (BMI >30.0 kg/m²). Twelve of the 29 subjects were insulin resistant based on a HOMA-IR value >2.5, but none of them had type 2 diabetes. This sample was specifically

TABLE 1. Anthropometric characteristics (n = 29)

Variables	Mean \pm SD	Range (Minimum–Maximum)
Age and anthropometrics		
Age (years)	48.1 \pm 4.1	40.4–54.5
Weight (kg)	76 \pm 17	53–133
Height (cm)	159 \pm 5	151–170
BMI (kg/m ²)	30.0 \pm 6.8	21.5–51.3
Waist circumference (cm) ^a	97.2 \pm 15.5	72.5–147.0
Total body fat mass (kg) ^a	28.8 \pm 8.9	12.4–50.4
Total lean body mass (kg) ^a	43.8 \pm 6.1	29.3–55.2
% fat ^a	37.6 \pm 5.8	23.3–48.6
Adipose tissue areas (cm ²)		
Total ^b	448 \pm 151	192–773
Subcutaneous ^b	340 \pm 128	129–555
Visceral	111 \pm 64	44–266
Adipocyte diameter (μ m)		
Subcutaneous ^a	104.0 \pm 11.4	77–131
Omental ^b	90.7 \pm 14.8	65–117
Cholesterol (mM) ^a		
Total	5.2 \pm 1.1	3.2–6.9
VLDL	0.5 \pm 0.2	0.4–0.6
LDL	3.3 \pm 0.9	1.3–4.7
HDL	1.4 \pm 0.3	0.8–2.1
Triglycerides (mM) ^a		
Total	1.4 \pm 0.6	0.7–2.5
VLDL	0.9 \pm 0.5	0.3–1.8
LDL	0.2 \pm 0.1	0.1–0.6
HDL	0.2 \pm 0.1	0.2–0.3
Glucose homeostasis		
Glucose (mM)	5.9 \pm 0.7	4.8–7.1
Insulin (μ U/ml)	11.4 \pm 4.4	3.3–45.3
HOMA-IR	2.4 \pm 1.3	0.7–13.7

HOMA-IR, homeostasis model assessment-insulin resistance.

^an = 28.

^bn = 27.

designed to identify cardiometabolic risk factors and adipose tissue dysfunction, features that relate to obesity and fat distribution in women.

Dietary CoQ10 consumption and smoking status

Using a food frequency questionnaire, we found that women included in our study consumed an average of 4.6 mg of CoQ10 per day with a range from 2.0 to 8.0 mg/day. BMI of the volunteers did not influence their daily consumption of CoQ10 from diet (supplementary Fig. 1A). We also found that vegetal sources (oils, nuts, vegetables, and fruits) were the main sources of CoQ10 in this French Canadian population (supplementary Fig. 1C). In this study, CoQ10 consumption did not influence the total levels and redox state of this molecule in the omental (supplementary Fig. 2A–C) or the subcutaneous (supplementary Fig. 2B–D) adipose tissue compartment. Only four volunteers were smokers and were distributed among BMI subgroups. We did not observe any specific pattern of CoQ10 content or redox state in adipose tissues of these individuals (data not shown).

Regional variation of CoQ10 in obesity

We were able to quantitatively assess the levels of CoQ10_{ox} and CoQ10_{red} in 24 omental and 22 subcutaneous samples. We excluded data from five omental (overweight, $n = 3$; obese, $n = 2$) and seven subcutaneous (lean, $n = 2$; overweight, $n = 4$; obese, $n = 1$) samples because of complete oxidation of the CoQ10_{red} isoform during the extraction process. We considered the CoQ10_{ox} levels as the CoQ10_{tot} pool for these samples. However, only women with available data of CoQ10_{ox}, CoQ10_{red}, and CoQ10_{tot} within the same depot were included in this set of analysis. We first analyzed the regional variation of CoQ10 content in lean, overweight, or obese patients. We did not observe a difference in CoQ10_{tot} content between the omental and subcutaneous adipose tissue of women within the same BMI category (Fig. 1A). However, we observed a depletion of the CoQ10 pool in omental adipose tissue of overweight and obese women, as well as in subcutaneous adipose tissue of obese women (BMI effect: $P = 0.001$; Fig. 1A). In lean individuals, we measured higher concentrations of the CoQ10_{red} isoform in the omental depot compared with subcutaneous tissue ($P = 0.003$; Fig. 1B). However, we found higher levels of CoQ10_{ox} isoform in subcutaneous adipose tissue of these women ($P = 0.01$; Fig. 1C). As expected, they displayed greater CoQ10 redox state in the subcutaneous depot (depot effect: $P = 0.0003$; Fig. 2A), suggesting that omental and subcutaneous adipose tissues have distinct CoQ10 redox statuses in healthy volunteers. The content in CoQ10_{red} was decreased specifically in omental adipose tissue of obese women ($P = 0.007$; Fig. 1B). A reduction in CoQ10_{ox} concentrations was also observed in subcutaneous adipose tissue of overweight and obese volunteers (Fig. 1C). Because of these differences, regional variations in CoQ10 redox state were not significant (Fig. 2A).

CoQ10 redox state and oxidative stress in abdominal adipose tissues

For samples with valid CoQ10 redox state data, 16 omental and 18 subcutaneous fat samples were available for LPO

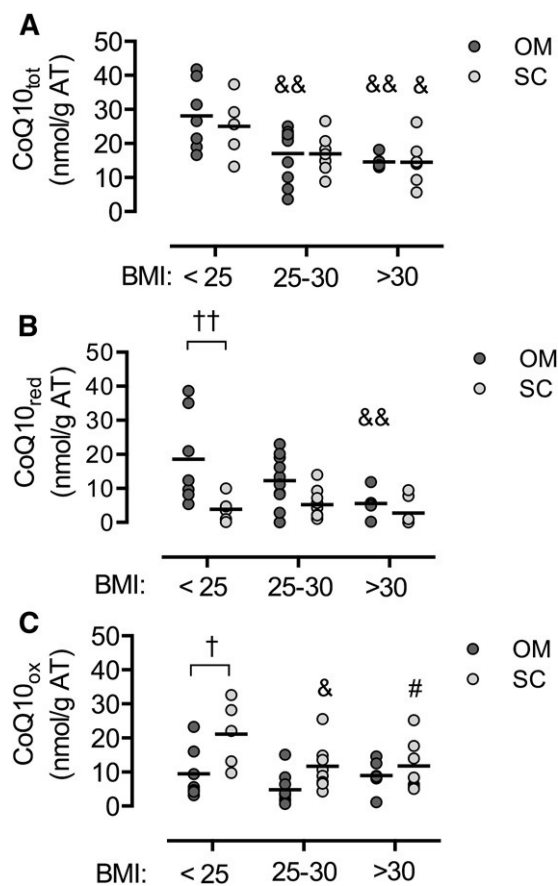


Fig. 1. Content in total (A), reduced (B), and oxidized (C) forms of CoQ10 per gram of omental and subcutaneous fat. The horizontal bar is the mean of the distribution. # $P \leq 0.10$, & $P \leq 0.05$, and && $P \leq 0.01$ versus lean subjects, † $P \leq 0.05$, †† $P \leq 0.01$, OM versus SC adipose tissues. Dark gray and light gray dots respectively represent OM and SC adipose tissue samples. OM ($n = 24$), SC ($n = 22$). OM, omental; SC, subcutaneous.

levels quantification as a marker of oxidative stress. The omental depot had higher levels of LPO than the subcutaneous compartment (depot effect: $P < 0.0001$; Fig. 2B). We also observed a significant increase in the omental LPO content of obese women compared with lean and overweight volunteers ($P = 0.01$ and 0.02 respectively; Fig. 2B). A positive association was found between the CoQ10 redox state and LPO content in omental adipose tissue ($r = 0.67$, $P = 0.005$; Fig. 2C), supporting a role of the CoQ10 redox state in the regulation of redox status and oxidative stress in visceral fat. However, the association between CoQ10_{tot} and LPO levels was not statically significant in this sample of patients ($r = -0.41$, $P = 0.11$). LPO concentration in subcutaneous adipose tissue was similar for all groups (Fig. 2B) and was not linked with the CoQ10 redox state (data not shown).

Influence of adipose tissue distribution and adipocyte diameter on CoQ10 content

Table 2 provides the Pearson and Spearman Rho values describing the correlations between adipose tissue areas measured by axial tomography and the abundance of CoQ10 isoforms in subcutaneous and omental adipose tissues. We found significant negative associations between

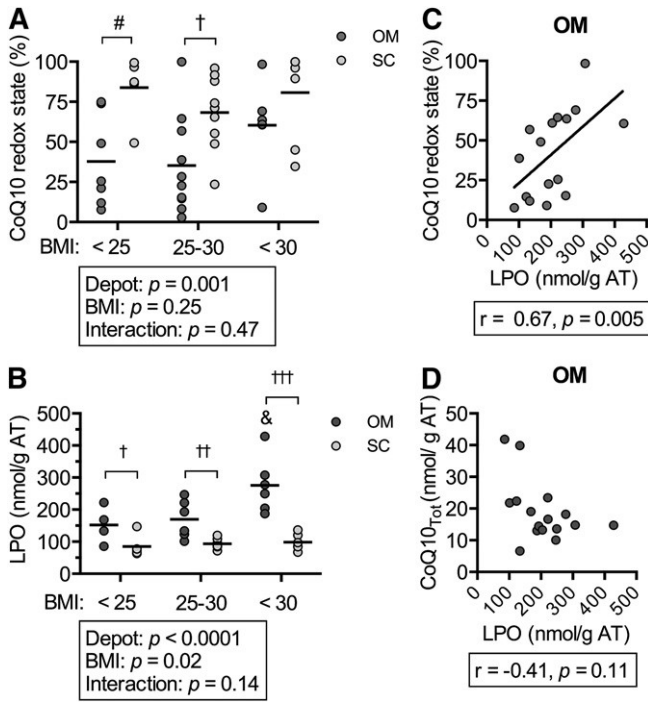


Fig. 2. Redox state of CoQ10 (A) and LPO levels (B) in the OM and SC compartment. Spearman correlation between LPO levels, CoQ10 redox state (C), and CoQ10 content (D) in the OM depot. The horizontal bar is the mean of the distribution. $^{\&}$ $P \leq 0.05$ body weight versus lean, $^{\#}$ $P = 0.06$, † $P \leq 0.05$, $^{++}$ $P \leq 0.01$, $^{+++}$ $P \leq 0.001$, OM versus SC adipose tissues. Dark gray and light gray dots respectively represent OM and SC adipose tissues samples. Redox state: OM ($n = 24$), SC ($n = 22$). LPO: OM ($n = 16$), SC ($n = 18$). OM, omental; SC, subcutaneous.

visceral ($r = -0.63, P = 0.0009$), subcutaneous ($r = -0.49, P = 0.02$), and total adipose tissue areas ($r = -0.58, P = 0.005$) with CoQ10_{red} levels in omental adipose tissue. Moreover, the CoQ10_{tot} pool negatively correlated with visceral ($r = -0.50, P = 0.006$), superficial subcutaneous ($r = -0.40,$

$P = 0.04$), and total ($r = -0.43, P = 0.02$) adipose tissue areas. The presence of the CoQ10_{ox} isoform in omentum was not associated with visceral or subcutaneous adiposity. The CoQ10 redox state of the visceral depot was also weakly associated with visceral adipose tissue area ($r = 0.37, P = 0.08$) and deep subcutaneous adipose tissue area ($r = 0.39, P = 0.07$). To test the hypothesis that visceral adipocyte hypertrophy is a major contributor to CoQ10 depletion in obesity, we adjusted the previous correlations for omental fat cell diameter. The association between omental CoQ10_{red} content and adipose tissue areas was no longer significant. Adjustment also abolished the relationship between the CoQ10_{tot} pool and visceral adipose tissue area, although the correlation with subcutaneous adipose tissue areas remained statistically significant ($r = -0.40, P = 0.05$).

Metabolic effects of low adipose tissue CoQ10 concentration

In a previous study, the concentration of 13.26 nmol of CoQ10 per gram of subcutaneous adipose tissue was identified as a phenotypic threshold value below which 95% of volunteers are obese (13). To quantify the metabolic effect of low and high CoQ10 content, we used a cutoff value of 14.0 and 15.0 nmol/g of subcutaneous and omental adipose tissues. This stratification generated two groups with either low or high CoQ10_{tot} concentrations within the same tissue (Fig. 3A–C). The women with low levels of CoQ10 in omental adipose tissue also displayed lower CoQ10_{red} concentrations ($P < 0.01$; Fig. 3A). The amount of CoQ10_{ox} (Fig. 3A) and the redox state (Fig. 3B) were not statistically different. Low CoQ10 content in the subcutaneous compartment was related to reduced CoQ10_{red} ($P = 0.02$) and CoQ10_{ox} ($P = 0.05$; Fig. 3C). The redox state (Fig. 3D) was similar in these subgroups.

Table 3 compares the anthropometric and metabolic characteristics of women with low versus high CoQ10 content in both tissues. As expected, volunteers with a lower

TABLE 2. Correlations between omental and subcutaneous adipose tissue content in CoQ10 and adipose tissue areas measured by CT

	Adipose Tissue Areas (cm ²)				
	Total	Visceral	Subcutaneous	Deep Subcutaneous	Superficial Subcutaneous
Omental content					
CoQ10 _{red}	-0.58 ^c	-0.63 ^d	-0.49 ^b	-0.51 ^b	-0.49 ^b
CoQ10 _{ox}	0.25	0.14	0.26	0.33	0.21
CoQ10 _{tot}	-0.43 ^b	-0.50 ^c	-0.35 ^a	-0.34 ^a	-0.40 ^b
% CoQ10 _{ox}	0.30	0.37 ^a	0.29	0.39 ^a	0.25
Omental content adjusted for omental adipocyte size					
CoQ10 _{red}	-0.18	-0.16	-0.33	-0.30	-0.30
CoQ10 _{ox}	-0.28	-0.18	-0.19	-0.23	-0.19
CoQ10 _{tot}	-0.30	-0.29	-0.40 ^b	-0.40 ^b	-0.37 ^a
% CoQ10 _{ox}	-0.05	-0.02	0.04	0.01	0.03
Subcutaneous content					
CoQ10 _{red}	-0.07	-0.19	0.01	-0.04	-0.04
CoQ10 _{ox}	-0.19	-0.12	-0.18	-0.21	-0.27
CoQ10 _{tot}	-0.15	0.03	-0.21	-0.21	-0.16
% CoQ10 _{ox}	-0.00	0.18	-0.11	-0.04	-0.05

^a $P \leq 0.10$.

^b $P \leq 0.05$.

^c $P \leq 0.01$.

^d $P \leq 0.001$.

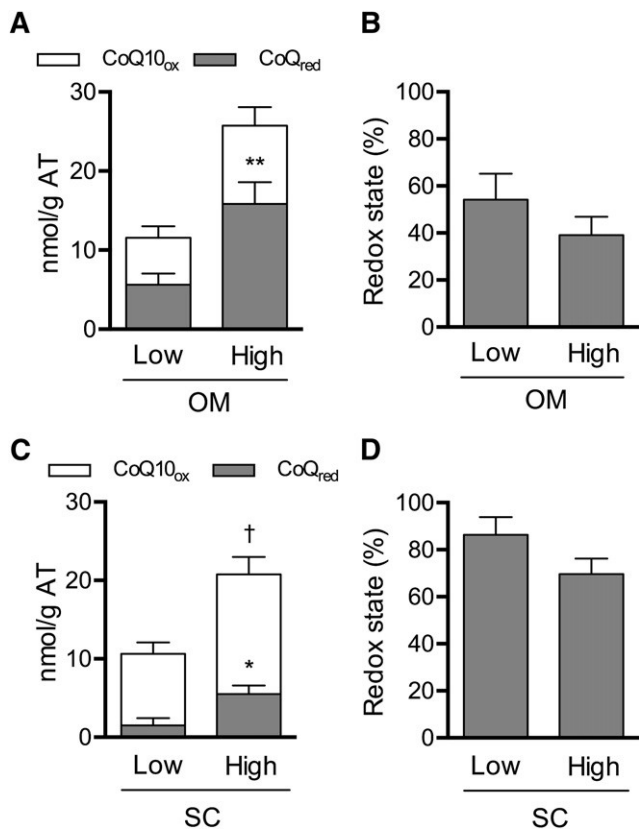


Fig. 3. Content in reduced, oxidized, and total forms of CoQ10 per gram of OM (A) and SC (C) fat in volunteers stratified by low or high CoQ10_{tot} content. CoQ10 redox state of the OM (B) and SC (D) depot was also determined. Data are means \pm standard error of the mean. * $P \leq 0.05$, ** $P \leq 0.01$; CoQ10_{red} content versus low CoQ10 groups, † $P \leq 0.05$; CoQ10_{ox} content low CoQ10 groups. White and gray bars respectively represent the oxidized and reduced isoforms of CoQ10. Low CoQ10 content group: OM (n = 9) and SC (n = 6). High CoQ10 content group: OM (n = 15), SC (n = 16). OM, omental; SC, subcutaneous.

amount of CoQ10 in the omental depot were more obese and had higher fat mass and fat-free mass. We also found higher visceral and subcutaneous adipose tissue areas, without differences in the visceral-to-subcutaneous area ratio. Even if they were more obese, these volunteers did not display any alteration in plasma lipid levels. However, an increase in mean omental adipocyte diameter, higher IL-6 and CRP plasma levels, and insulin resistance were observed. On the other hand, the group of women with lower CoQ10 content in subcutaneous adipose tissue was not characterized by higher adiposity or changes in body fat distribution. We did not observe any variation of the metabolic parameters except for fasting glucose level, which was slightly higher in women with higher CoQ10 content. We did not find any statistically significant variation of insulin levels or HOMA-IR index in these subgroups.

DISCUSSION

Most of the studies that investigated the link between CoQ10 and cardiometabolic health have focused on plasma

levels of this molecule. The circulating pool of CoQ10 is mostly found in high- and low-density lipoproteins, where it fulfills antioxidant roles (12). The redox state is often used as a marker of oxidative stress and has been shown to be higher in patients with type 2 diabetes (21). In this study, we examined the regional variations of CoQ10 content and redox state in two adipose tissue depots. We showed for the first time that CoQ10 redox state was fundamentally different among the omental and subcutaneous adipose tissues of lean individuals, despite similar total content. Indeed, we found that the omental depot displayed lower redox state, which is mainly driven by the high content in CoQ10_{red}. In lean and healthy women, regional variations of these parameters were not linked to adipocyte hypertrophy or inflammation, suggesting physiological variation of CoQ10 redox status between the intra-abdominal and subcutaneous adipose compartments. We also ruled out the contribution of CoQ10 from food as a major contributor of the adipose CoQ10 pool. Indeed, we established the daily consumption of CoQ10 between 2 and 8 mg/day in this sample of the French Canadian population. These results are similar to a previous study that reported a consumption of 3 to 5 mg of CoQ10 per day in a sample of Danish individuals (22). However, no association was found between dietary intake and adipose tissue CoQ10 content, suggesting that the intracellular levels may derive mainly from endogenous production.

We also observed that overweight volunteers had a reduced CoQ10_{tot} pool in omental adipose tissue, without modification of the redox state or lipid peroxidation. However, obese women displayed lower concentrations of CoQ10_{tot} with reduced levels of the antioxidant isoform (CoQ10_{red}) and greater LPO content. This indirectly suggests that the depletion in CoQ10 alone is not sufficient to trigger a sustained oxidative stress response. Nevertheless, CoQ10_{red} levels and the lower redox state observed in obese women are closely related to LPO production in omental adipose tissue. We can hypothesize that depletion of the CoQ10_{tot} pool measured in overweight volunteers may predispose omental adipocytes to oxidative damage in response to metabolic stress occurring mostly in obesity. Based on this assumption, a cohort of overweight patients with severe metabolic dysfunctions might also display impaired CoQ10 redox status and oxidative stress in the omental depot.

The loss of omental content in CoQ10 and CoQ10_{red} was strongly associated with both visceral and subcutaneous fat accumulation. Our results also indirectly suggest that hypertrophic remodeling of the visceral depot plays a critical role in this phenomenon. Moreover, we did not observe any difference in plasma lipids among women with low or high levels of CoQ10 in the omentum, suggesting that modification of CoQ10_{tot} content is not related to dyslipidemia. However those participants with low CoQ10 content displayed higher IL-6 and CRP plasma levels, suggesting early adipose tissue dysfunction. This group of participants also displayed insulin resistance and hyperinsulinemia without dysglycemia. Taken together, our results suggest that CoQ10 depletion and oxidative stress

TABLE 3. Anthropometric and metabolic parameters of women with low versus high CoQ10 content in omental and subcutaneous adipose tissues

	Omental Adipose Tissue ^a			Subcutaneous Adipose Tissue ^b		
	Low CoQ10 _{tot} (n = 11)	High CoQ10 _{tot} (n = 18)	<i>P</i>	Low CoQ10 _{tot} (n = 12)	High CoQ10 _{tot} (n = 17)	<i>P</i>
Body composition						
BMI (kg/m ²)	34.7 ± 2.4	27.2 ± 0.9	0.002	29.6 ± 1.8	30.4 ± 1.8	0.60
Fat mass (kg)	34.8 ± 2.6	25.5 ± 1.8	0.009	29.7 ± 2.9	28.2 ± 2.1	0.69
Lean body mass (kg)	47.1 ± 1.6	41.9 ± 1.4	0.02	42.7 ± 1.8	44.6 ± 1.5	0.44
Percentage of fat (%)	40.9 ± 1.3	35.7 ± 1.4	0.01	39.0 ± 1.4	36.5 ± 1.6	0.26
Adipose tissue areas (cm²)						
Total	554.7 ± 45.4	394.3 ± 30.6	0.01	428.1 ± 37.4	461.4 ± 42.3	0.56
Visceral	159.4 ± 21.5	81.8 ± 8.3	0.002	102.3 ± 18.5	117.6 ± 15.6	0.60
Subcutaneous	409.2 ± 37.2	305.2 ± 29.1	0.04	321.5 ± 32.6	352.6 ± 35.3	0.52
Deep subcutaneous	215.7 ± 21.1	155.8 ± 17.8	0.04	171.5 ± 19.2	181.5 ± 21.5	0.73
Superficial subcutaneous	205.2 ± 20.2	156.2 ± 12.5	0.06	174.8 ± 15.1	171.1 ± 16.6	0.87
Cholesterol (mM)						
Total	4.9 ± 0.3	5.3 ± 0.3	0.30	5.3 ± 0.3	5.0 ± 0.2	0.52
LDL	2.8 ± 0.3	3.1 ± 0.2	0.35	3.0 ± 0.3	2.9 ± 0.2	0.74
HDL	1.4 ± 0.1	1.6 ± 0.1	0.25	1.6 ± 0.1	1.5 ± 0.1	0.50
Triglycerides (mM)						
Total	1.4 ± 0.5	1.3 ± 0.1	0.39	1.4 ± 0.2	1.3 ± 0.1	0.58
Glucose homeostasis						
Glucose (mM)	6.0 ± 0.2	5.8 ± 0.2	0.45	5.6 ± 0.1	6.1 ± 0.2	0.05
Insulin (μU/ml)	15.0 ± 3.3	9.2 ± 1.0	0.04	9.7 ± 1.2	12.6 ± 2.3	0.42
HOMA-IR	4.1 ± 1.0	2.4 ± 0.3	0.04	2.5 ± 0.3	3.5 ± 0.7	0.31
Adiponectin and cytokines						
Adiponectin (pg/ml)	10.9 ± 1.4	10.9 ± 1.1	0.99	9.8 ± 1.3	11.6 ± 1.1	0.31
IL-6 (pg/ml)	1.3 ± 0.2	0.8 ± 0.1	0.03	0.9 ± 0.2	1.1 ± 0.1	0.18
CRP (mg/ml)	3.5 ± 0.9	1.3 ± 0.3	0.007	1.9 ± 0.7	2.4 ± 0.6	0.56
Adipocyte diameter (μm)						
Omental	98.5 ± 4.4	85.2 ± 3.4	0.03	90.9 ± 4.2	89.5 ± 4.2	0.81
Subcutaneous	108.8 ± 4.4	100.5 ± 1.8	0.14	101.1 ± 1.3	105.3 ± 3.6	0.28

CRP, C-reactive protein; IL-6, interleukin-6. Bold *P* values are statistically significant.

^aCutoff value of 15 nmol/g of adipose tissue.

^bCutoff value of 14 nmol/g of adipose tissue.

might be involved in visceral adipose tissue dysfunction leading to insulin resistance and increased risk of developing type 2 diabetes.

Surprisingly, we did not find any difference in CoQ10 concentrations in the subcutaneous adipose tissues of overweight versus obese individuals. A previous study found a reduction of CoQ10 levels in subcutaneous samples from obese (BMI from 31 to 40 kg/m²) and morbidly obese (BMI >40 kg/m²) men and women, compared with lean individuals (13). In that study, overweight patients displayed CoQ10 content that was similar to that of lean volunteers. The conclusion drawn from the latter investigation differs from this work, but could be explained by the nature of the population studied. Most of the women included in the present study had a BMI <40 kg/m². The relation between mean adipocyte size and adiposity level is mostly linear in the subcutaneous depot, until it reaches a plateau in very obese women [reviewed in (23)]. This suggests that most patients included in our investigation still had an important potential for hypertrophic remodeling of the subcutaneous depot despite their excess of body fat mass. If we assume that adipocyte hypertrophy has the same effect on CoQ10 in fat from all anatomical locations, it is possible that adipocyte dysfunction associated with CoQ10 depletion only occurs in females with very high BMI values. We observed a specific and significant reduction of the CoQ10_{ox} content in overweight and obese volunteers, without any variation of CoQ10_{red} levels or redox state. However, this decrease in CoQ10_{ox} levels was not

related to lipid peroxidation. Moreover, the metabolic profile of participants with low versus high CoQ10 content in subcutaneous adipose tissue was similar between groups. Despite variation in the absolute CoQ10_{red} and CoQ10_{ox} levels, we did not observe modifications in plasma lipid levels, insulin resistance, and cytokine secretion. This suggests that the lipophilic antioxidant system in subcutaneous adipose tissue is not a major factor influencing metabolic health of women with moderate obesity. Other antioxidant enzymes like catalase, manganese-dependent SOD, or GPx might be involved in the regulation of the intracellular redox status. Indeed, obese Zucker rats had reduced activity of these enzymes in the inguinal fat pad (2).

The CoQ10 redox state might have different physiological significance depending on the cellular localization on the CoQ10 pool in adipocytes. During mitochondrial respiration, the CoQ10_{ox} is reduced by complex I or II and carries electrons to complex III. At high mitochondrial membrane potential, a low CoQ10 redox state promotes ROS production. Indeed, higher levels of CoQ10_{red} in mitochondrial membranes promotes the formation of reactive semiquinone radicals at the Q-binding site of complex I [reviewed in (7)]. The CoQ10 redox state also favors ROS production at the Q_o site of the complex III under proper circumstances. On the other hand, ROS derived from complex III are released in the intermembrane space (7). They can diffuse directly in the cytosol and may act as “signaling ROS” to trigger adaptive responses to oxidative stress. Primary cultures of skin fibroblasts isolated from

patients harboring *COQ2* and *PDSS2* mutations displayed defects in ATP synthesis and oxidative damage (24). Otherwise, the CoQ10_{red} in other cellular membranes displayed antioxidant effects.

The cross-sectional and retrospective nature of this study leads to several technical limitations. We were not able to specifically measure the CoQ10 content and redox state in separate cell compartments. Moreover the depletion of the CoQ10 pool might affect mitochondrial metabolism and ROS production only under specific metabolic conditions. We could not exclude that defects in mitochondrial function could occur in the postprandial state instead of fasting. Moreover the population studied only included a relatively small sample of Caucasian women from 40 to 55 years of age. These results cannot be extrapolated to cohorts of men, pediatric or adolescent obese individuals, and other ethnic groups. Further studies should be conducted to clarify the importance of this phenomenon in the general population.

CONCLUSION

Hypertrophic remodeling of the omental fat depot is related to a smaller CoQ10 pool, which is mostly explained by loss of the antioxidant isoform (CoQ10_{red}, ubiquinol). This phenomenon is associated with the presence of oxidative stress markers in this depot, systemic low-grade inflammation, and insulin resistance. However, it was not directly linked to dyslipidemia in this sample of healthy women, suggesting that modifications of the CoQ10 redox state and content might be an early mechanism leading to visceral fat dysfunction. 

The authors would like to acknowledge the essential contribution of the study coordinator, gynecologists, nurses, and radiology technicians of Laval University Medical Research Center, as well as the collaboration of participants.

REFERENCES

- Carpentier, A. C., S. M. Labbé, T. Grenier-Larouche, and C. Noll. 2011. Abnormal dietary fatty acid metabolic partitioning in insulin resistance and type 2 diabetes. *Clin. Lipidol.* **6**: 703–716.
- Furukawa, S., T. Fujita, M. Shimabukuro, M. Iwaki, Y. Yamada, Y. Nakajima, O. Nakayama, M. Makishima, M. Matsuda and I. Shimomura. 2004. Increased oxidative stress in obesity and its impact on metabolic syndrome. *J. Clin. Invest.* **114**: 1752–1761.
- Wang, Z., X. Dou, D. Gu, C. Shen, T. Yao, V. Nguyen, C. Braunschweig and Z. Song. 2012. 4-hydroxynonenal differentially regulates adiponectin gene expression and secretion via activating PPARgamma and accelerating ubiquitin-proteasome degradation. *Mol. Cell. Endocrinol.* **349**: 222–231.
- Zhang, X., Z. Wang, J. Li, D. Gu, S. Li, C. Shen and Z. Song. 2013. Increased 4-hydroxynonenal formation contributes to obesity-related lipolytic activation in adipocytes. *PLoS One.* **8**: e70663.
- Ingram, K. H., H. Hill, D. R. Moellering, B. G. Hill, C. Lara-Castro, B. Newcomer, L. J. Brandon, C. P. Ingalls, M. Penumetcha, J. C. Rupp et al. 2012. Skeletal muscle lipid peroxidation and insulin resistance in humans. *J. Clin. Endocrinol. Metab.* **97**: E1182–E1186.
- Pillon, N. J., M. L. Croze, R. E. Vella, L. Souler, M. Lagarde, and C. O. Soulage. 2012. The lipid peroxidation by-product 4-hydroxy-2-nonenal (4-HNE) induces insulin resistance in skeletal muscle through both carbonyl and oxidative stress. *Endocrinology.* **153**: 2099–2111.
- Dröse, S., and U. Brandt. 2012. Molecular mechanisms of superoxide production by the mitochondrial respiratory chain. *Adv. Exp. Med. Biol.* **748**: 145–169.
- Fernández-Ayala, D. J., G. Brea-Calvo, G. Lopez-Lluch, and P. Navas. 2005. Coenzyme Q distribution in HL-60 human cells depends on the endomembrane system. *Biochim. Biophys. Acta.* **1713**: 129–137.
- Littarru, G. P., and L. Tiano. 2007. Bioenergetic and antioxidant properties of coenzyme Q10: recent developments. *Mol. Biotechnol.* **37**: 31–37.
- Morré, D. J., and D. M. Morre. 2011. Non-mitochondrial coenzyme Q. *Biofactors.* **37**: 355–360.
- Crane, F. L., I. L. Sun, M. G. Clark, C. Grebing, and H. Low. 1985. Transplasma-membrane redox systems in growth and development. *Biochim. Biophys. Acta.* **811**: 233–264.
- Mohr, D., V. W. Bowry, and R. Stocker. 1992. Dietary supplementation with coenzyme Q10 results in increased levels of ubiquinol-10 within circulating lipoproteins and increased resistance of human low-density lipoprotein to the initiation of lipid peroxidation. *Biochim. Biophys. Acta.* **1126**: 247–254.
- Bour, S., M. C. Carmona, A. Galinier, S. Caspar-Bauguil, L. Van Gaal, B. Staels, L. Pénicaud, and L. Casteilla. 2011. Coenzyme Q as an antiadipogenic factor. *Antioxid. Redox Signal.* **14**: 403–413.
- Michaud, A., R. Drolet, S. Noel, G. Paris, and A. Tchernof. 2012. Visceral fat accumulation is an indicator of adipose tissue macrophage infiltration in women. *Metabolism.* **61**: 689–698.
- Michaud, A., M. Pelletier, S. Noël, C. Bouchard, A. Tchernof. 2013. Markers of macrophage infiltration and measures of lipolysis in human abdominal adipose tissues. *Obesity (Silver Spring).* **21**: 2342–2349.
- Rodbell, M. 1964. Metabolism of isolated fat cells. I. effects of hormones on glucose metabolism and lipolysis. *J. Biol. Chem.* **239**: 375–380.
- Deschênes, D., P. Couture, P. Dupont, and A. Tchernof. 2003. Subdivision of the subcutaneous adipose tissue compartment and lipid-lipoprotein levels in women. *Obes. Res.* **11**: 469–476.
- Galiniere, A., A. Carriere, Y. Fernandez, A. M. Bessac, S. Caspar-Bauguil, B. Periquet, M. Comtat, J. P. Thouvenot and L. Casteilla. 2004. Biological validation of coenzyme Q redox state by HPLC-EC measurement: relationship between coenzyme Q redox state and coenzyme Q content in rat tissues. *FEBS Lett.* **578**: 53–57.
- Goulet, J., G. Nadeau, A. Lapointe, B. Lamarche, and S. Lemieux. 2004. Validity and reproducibility of an interviewer-administered food frequency questionnaire for healthy French-Canadian men and women. *Nutr. J.* **3**: 13.
- Pravst, I., K. Zmitek, and J. Zmitek. 2010. Coenzyme Q10 contents in foods and fortification strategies. *Crit. Rev. Food Sci. Nutr.* **50**: 269–280.
- Lim, S. C., H. H. Tan, S. K. Goh, T. Subramaniam, C. F. Sum, I. K. Tan, B. L. Lee, and C. N. Ong. 2006. Oxidative burden in prediabetic and diabetic individuals: evidence from plasma coenzyme Q(10). *Diabet. Med.* **23**: 1344–1349.
- Weber, C., A. Bysted, and G. Hillmer. 1997. The coenzyme Q10 content of the average Danish diet. *Int. J. Vitam. Nutr. Res.* **67**: 123–129.
- Tchernof, A., and J. P. Despres. 2013. Pathophysiology of human visceral obesity: an update. *Physiol. Rev.* **93**: 359–404.
- Quinzii, C. M., L. C. Lopez, J. Von-Moltke, A. Naini, S. Krishna, M. Schuelke, L. Salviati, P. Navas, S. DiMauro, and M. Hirano. 2008. Respiratory chain dysfunction and oxidative stress correlate with severity of primary CoQ10 deficiency. *FASEB J.* **22**: 1874–1885.